

recent theoretical findings in highly condensed DNA phases (41). The observed quantitative control over the structural nature of the DNA packing in CL-DNA complexes may lead to a better understanding of the important structural parameters relevant to transfection efficiencies in gene therapy (26); in particular, they should be directly relevant to our understanding of the interactions of the complex with cellular lipids and the mechanism of DNA transfer across the nuclear membrane.

REFERENCES AND NOTES

- R. G. Crystal, *Science* **270**, 404 (1995); R. C. Mulligan, *ibid.* **260**, 926 (1993).
- P. L. Felgner and G. Rhodes, *Nature* **349**, 351 (1991); J.-P. Behr, *Bioconj. Chem.* **5**, 382 (1994); A. Singhal and L. Huang, *Gene Therapeutics: Methods and Applications of Direct Gene Transfer*, J. A. Wolff, Ed. (Birkhauser, Boston, 1994).
- P. L. Felgner *et al.*, *Proc. Natl. Acad. Sci. U.S.A.* **84**, 7413 (1987).
- N. Zhu, D. Liggitt, Y. Liu, R. Debs, *Science* **261**, 209 (1993).
- G. J. Nabel *et al.*, *Proc. Natl. Acad. Sci. U.S.A.* **90**, 11307 (1993); N. M. Caplen *et al.*, *Nature Med.* **1**, 39 (1995).
- D. Lasic and N. S. Templeton, *Adv. Drug Deliv. Rev.*, in press.
- E. Marshall, *Science* **269**, 1050 (1995); *ibid.* **270**, 1751 (1995).
- V. A. Bloomfield, *Biopolymers* **31**, 1471 (1991).
- F. Livolant, A. M. Levelut, J. Doucet, J. P. Benoit, *Nature* **339**, 724 (1989).
- Z. Reich, E. J. Wachtel, A. Minsky, *Science* **264**, 1460 (1994).
- E. Sackmann, *ibid.* **271**, 43 (1996); C. Ligoure, G. Bouglet, G. Porte, *Phys. Rev. Lett.* **71**, 3600 (1993).
- H. E. Warriner, S. H. J. Idziak, N. L. Slack, P. Davidson, C. R. Safinya, *Science* **271**, 969 (1996); A. K. Kemworthy, K. Hristova, D. Needham, T. J. McIntosh, *Biophys. J.* **68**, 1921 (1995).
- H. Gershon, R. Ghirlando, S. B. Guttman, A. Minsky, *Biochemistry* **32**, 7143 (1993).
- J. Gustafsson, G. Arvidson, G. Karlsson, M. Almgren, *Biochim. Biophys. Acta* **1235**, 305 (1995).
- B. Sternberg, F. L. Sorgi, L. Huang, *FEBS Lett.* **356**, 361 (1994).
- S. B. Smith, L. Finzi, C. Bustamante, *Science* **258**, 1122 (1992); T. T. Perkins, D. E. Smith, S. Chu, *ibid.* **264**, 819 (1994).
- A mixture of DOPE/DOTAP (1:1, wt:wt) was prepared in a 20-mg/ml chloroform stock solution; 500 ml was dried under nitrogen in a narrow glass beaker and desiccated under vacuum for 6 hours. After addition of 2.5 ml of Millipore water and 2 hours incubation at 40°C, the vesicle suspension was sonicated to clarity for 10 min. The resulting solution of liposomes (25 mg/ml) was filtered through 0.2- μ m Nucleopore filters. For optical measurements, the concentration of SUV used was between 0.1 and 0.5 mg/ml. All the lipids were purchased from Avanti Polar Lipids, Inc. (Alabaster, AL).
- The liposome and complex sizes were measured by dynamic light scattering (Microtrac UPA 150, Leeds and Northrup).
- Purified λ -phage DNA and pBR322 plasmid were purchased from Biolabs, New England. Optical and x-ray data were taken with linear λ prepared in two ways: (i) used as delivered, and (ii) by heating to 65°C and reacting with a surplus of a 12-base oligo complementary to the 3' COS end. Subsequently, the DNA was ligated (T4 DNA ligase, Fischer). The methods gave the same result. For the optical experiments, the DNA concentration used was between 0.01 and 0.1 mg/ml.
- A Nikon Diaphot 300 equipped for epifluorescence and high-resolution DIC was used.
- Sonicated DOPE-DOTAP (1:1) liposomes were pre-

- pared at 0.1 mg/ml with 0.2 mol % DHPE-Texas Red fluorescence label. DNA stained by YOYO (Molecular Probes) was added under gentle mixing at different L/D s.
- J. O. Rädler, I. Koltov, T. Salditt, A. Jamieson, C. R. Safinya, unpublished results.
 - High-resolution synchrotron x-ray scattering was performed at the Stanford Synchrotron Radiation Laboratory. Lower resolution XRD experiments were performed with a rotating anode source.
 - The DNA-lipid condensates were prepared from a 25-mg/ml liposome suspension and a 5-mg/ml DNA solution. The solutions were filled in 2-mm-diameter quartz capillaries with different ratios L/D , respectively, and mixed after flame sealing by gentle centrifugation up and down the capillary.
 - A. Lin, N. Slack, S. H. J. Idziak, C. R. Safinya, unpublished results.
 - The intercalation of λ -DNA between membranes in CL-DNA complexes was found to protect it against a Hind III restriction enzyme, which cuts naked λ -DNA at seven sites (22).
 - D. Roux and C. R. Safinya, *J. Phys. (France)* **49**, 307 (1988).
 - C. R. Safinya, in *Phase Transitions in Soft Condensed Matter*, R. Tormod and D. Sherrington, Eds. (Plenum, New York, 1989), pp. 249–270.
 - R. Podgornik, D. C. Rau, V. A. Parsegian, *Macromolecules* **22**, 1780 (1989).
 - The multilamellar structure of the complex (with λ -DNA) and the distinct DNA interhelical packing regimes were also found in SAXS data in binary mixtures of cationic lipids that contained DOPE [which has a high transfection efficiency (2)] as the neutral colipid. However, the complexes showed a phase separation into two condensed phases.
 - G. S. Manning, *J. Chem. Phys.* **51**, 924 (1969).
 - P. Boltenhagen, O. D. Lavrentovich, M. Kleman, *Phys. Rev. A* **46**, 1743 (1992).
 - The projected charge density of DNA (two anionic

charges per 68 Å²) is nearly matched by two cationic head groups on DOTAP of ~70 Å² each and thus permits near complete neutralization of the complex (Fig. 3A).

- The variation in the interlayer spacing d ($= \delta_w + \delta_m$) (Fig. 4B) arises from the increase in the membrane bilayer thickness δ_m as L/D increases (each DOPC molecule is ~4 to 6 Å longer than a DOTAP molecule). δ_m was obtained at each L/D by measuring d in the L_α phase multilayer membranes at the corresponding DOTAP to DOPC ratio and using the relation $\delta_m = d(1 - \Phi_w)$, Φ_w = water volume fraction. The measured δ_m and d , gave $\delta_w = 25 \pm 1.5$ Å, close to the spacing for the DNA monolayer (see Fig. 3A).
- I. Kolover, T. Salditt, J. Rädler, C. R. Safinya, unpublished results.
- J. V. Selinger and R. F. Bruinsma, *Phys. Rev. A* **43**, 2922 (1991).
- W. Helfrich, *Z. Naturforsch. Teil A* **33**, 305 (1978).
- C. R. Safinya *et al.*, *Phys. Rev. Lett.* **57**, 2718 (1986).
- E. A. Evans and V. A. Parsegian, *Proc. Natl. Acad. Sci. U.S.A.* **83**, 7132 (1986).
- N. Dan, *Biophys. J.*, in press.
- R. D. Kamien and D. R. Nelson, *Phys. Rev. E* **53**, 650 (1996).
- We acknowledge useful discussions with R. Bruinsma, N. Dan, W. Gelbart, P. Pincus, J. Prost, T. Lubensky, and D. Lasic. Supported in part by NSF grant DMR-9624091, the Petroleum Research Fund (31352-AC7), and a Los Alamos CULAR grant STB/UC:96-108. J.O.R. and T.S. acknowledge partial support by DFG (Ra 655/1-1) and DAAD scholarships, respectively. The Materials Research Laboratory at Santa Barbara is supported by the NSF under grant DMR-9632716. The synchrotron experiments were carried out at Stanford (SSRL) supported by the U.S. Department of Energy.

17 July 1996; accepted 24 October 1996

The Water Dipole Moment in Water Clusters

J. K. Gregory, D. C. Clary,* K. Liu, M. G. Brown, R. J. Saykally

The average dipole moment of a water molecule in the condensed phase is enhanced by around 40 percent relative to that of an isolated monomer. This enhancement results from the large polarization caused by the electric field induced by surrounding monomers. A quantitative molecular description of this polarization is essential for modeling aqueous solvation phenomena. This combined theoretical and experimental study of dipole moments in small water clusters provides such a description and also gives insights into the structure of liquid water.

Water clusters have been studied extensively both experimentally (1) and theoretically (2–4) in recent years. Their study provides a means of systematically explaining the properties of the bulk liquid, which exists as an extended and dynamic hydrogen-bonded network (5). The research area has witnessed rapid advances as a result of new experimental and computational techniques (6). The ultimate goals are the de-

velopment of an accurate many-body potential energy surface (PES) that describes the electronic energy of a system of interacting water molecules and of a quantitative description of the condensed phases of water (7).

The dipole moment of an isolated water monomer is 1.855 D (8), whereas the corresponding value in the condensed phase increases from 2.4 to 2.6 D as a result of polarization by the environment (9) (the debye unit $D = 3.336 \times 10^{-30}$ C/m). Theoretical treatments based on ice lattices have suggested even higher values of about 3.0 D (10). Simulations of condensed water based on the use of pairwise additive potentials generally require exaggerated mono-

J. K. Gregory, Department of Chemistry, University of Cambridge, Cambridge CB2 1EW, UK.

D. C. Clary, Department of Chemistry, University College London, London WC1H 0AJ, UK.

K. Liu, M. G. Brown, R. J. Saykally, Department of Chemistry, University of California, Berkeley, CA 94720, USA.

*To whom correspondence should be addressed.

mer dipoles of 2.3 to 2.4 D to reproduce experimental data (11, 12), and the increase in dipole moment on going from the gas to the condensed phase can only be accurately described if polarizability is accounted for explicitly. *Ab initio* molecular dynamics calculations yield a value of 2.66 D for the liquid water case (12). A recent calculation based on the use of a coupled density functional–molecular mechanics Hamiltonian to simulate a quantum water molecule in a classical system gave large fluctuations of the instantaneous value of the dipole moment of the quantum molecule (13).

In the theoretical part of this work, we used high-level *ab initio* calculations (14) to calculate the dipole moments of the individual molecules (monomers) in water clusters ranging from dimers to octamers. The individual calculation of the dipoles was facilitated by a distributed multipole analysis (15), which allows local multipoles to be obtained at a variety of sites in a molecule. In the *ab initio* calculations on water clusters reported here, we used aug-cc-VDZ basis sets (16) and second-order Møller-Plesset perturbation theory (MP2) (17) to take into account electron correlation effects. It has been shown that MP2 calculations with a similar basis set give good accuracy for the properties of water clusters (18).

These calculations give an isolated monomer dipole of 1.868 D, which is within 1% of the value observed experimentally

(8). To calculate the contributions to the total dipole moments of the water dimer, trimer, tetramer, and pentamer, we considered only the most stable structures (Fig. 1A). The calculated *a*-dipole component of the water dimer, $\mu_a = 2.683$ D, is close to the experimental value of 2.643 D (19) [the projection (μ_a) of the total dipole moment along the *a*-inertial axis of the near prolate rotor essentially passes through the two O atoms in the dimer]. The calculated values for the trimer and pentamer dipoles are 1.071 and 0.927 D, respectively. The symmetry of the tetramer ensures that its dipole moment is zero.

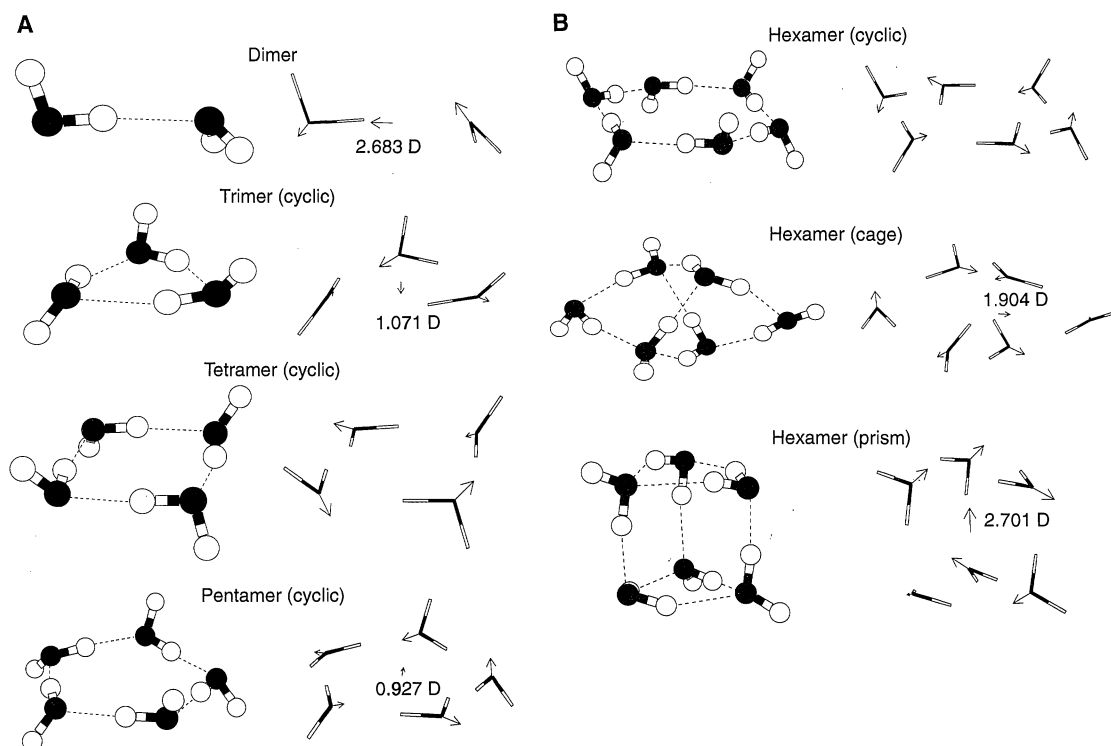
The water hexamer represents a cross-over point, where noncyclic structures become more stable than cyclic ones. Recent theory and experiment (20) have suggested that the most stable form of the water hexamer is a “cage” structure with eight hydrogen bonds (Fig. 1B). We also considered two further hexamer structures, namely, the prism and cyclic structures, which are known to be almost isoenergetic with the cage isomer (21). The prism is probably the global minimum on the hexamer electronic PES (21), whereas a smaller vibrational zero-point energy is responsible for the greater stability of the cage (20), and the cyclic structure is of further interest because of its similarity to the structure of ice I_h . The cyclic hexamer, like the tetramer, has no overall dipole moment because of its symmetry.

To evaluate the accuracy of the theoret-

ical predictions, we used terahertz laser vibration-rotation-tunneling (VRT) spectroscopy (22, 23) to measure explicitly the electric dipole moment of the cage hexamer from the Stark effect of its VRT transitions. First-order spectral splittings induced by the electric field enabled us to determine μ_a . From the fully resolved $\Delta M = 0$ and $\Delta M = \pm 1$ Stark features of the $P(4)$ transition (Fig. 2), we obtained the *a*-dipole components $\mu_a'' = 1.85$ D and $\mu_a' = 1.89$ D, with the double prime denoting the ground state and single prime the vibrationally excited state. To remove the correlation in μ_a between the ground and excited states, we considered the fully resolved $\Delta M = \pm 1$ transitions of the $P(4)$ line in conjunction with the $\Delta M = 0$ ones in the dipole determination.

We calculated Stark energies and transition frequencies using the expressions appropriate for nearly degenerate asymmetry doubling, which should exhibit first-order behavior for the states of quantum number $K_a \geq 3$ according to the rotational energy levels established for the cage in our earlier experiment (20). Tunneling splittings are not affected by the electric field, because the interactions among different nuclear spin states through the external field become symmetry-forbidden at least to the first order in this case. We synthesized the simulated line shape in Fig. 2 by twice differentiating the superimposed Gaussian profiles (2.1 MHz full width at half maximum) that are centered on the predicted line positions. On the basis of the peak

Fig. 1. (A) Lowest energy structures of the water dimer, trimer, tetramer, and pentamer with dotted lines at left corresponding to hydrogen bonds. The individual dipoles on each monomer are shown on the right as arrow vectors pointing away from each O atom. Also shown are the direction and magnitude of the total dipole moment of the cluster. For the tetramer, the total dipole moment is zero as a result of S_4 symmetry. (B) Three structures of the water hexamer together with their dipole moments. The cyclic structure, like the tetramer, has no net dipole moment because it has S_6 symmetry.



positions of the calculated spectrum rather than the stick frequencies, a nonlinear least squares fit of the field-dependent peak separations was performed to yield μ_a'' and μ_a' . Other partially resolved transitions exhibiting the first-order Stark effect were also analyzed. A strong dependence of both μ_a'' and μ_a' on the quantum numbers J and K_a was found to produce values ranging from 1.82 to 2.07 D. Aside from the true quantum and vibrational excitation effects, these large variations are caused by the difficulties in uniquely reproducing the unresolved features and in calibrating the electric field, leading to a percentage error in μ_a of less than 5%. Furthermore, from the observed Stark splitting patterns, we can determine that μ_a'' and μ_a' have the same signs.

Stark measurements were also attempted for $(\text{H}_2\text{O})_3$, $(\text{D}_2\text{O})_3$, $(\text{D}_2\text{O})_4$, and $(\text{D}_2\text{O})_5$, but no spectral splitting or broadening was observed at the highest electric field strength (~ 45 V/cm) attainable in our apparatus. A plausible explanation is that low-barrier facile out-of-plane flipping motions of the free O-H or O-D bonds effectively average the overall cluster dipoles to zero

despite their appreciable values at the equilibrium geometries as predicted for the asymmetric trimer and pentamer in the above ab initio calculations. The dynamic symmetry (containing the space inversion) caused by flipping requires the vibrationally averaged permanent dipole moments to average to zero for the cyclic trimer and pentamer, as in the ammonia monomer and dimer wherein the permanent dipole averages to zero because of the umbrella inversion (24).

To complement our ab initio calculations and to rationalize the origin of the a axis dipole component for the cage hexamer, we also modeled the dipole moments using an induction expansion through the dipole- and quadrupole-induced dipole terms; we solved the induced electric field in an iterative self-consistent manner using the known anisotropic polarizability (25) and quadrupole moments (26) of the monomer. The structures from the dimer to hexamer used in this model were derived consistently from the experimental rotational constants. Using this model for the dimer, we obtained a μ_a of 2.61 D, which is in

agreement with the experimental value (19). For the cage hexamer μ_a is 2.02 D, which is in reasonable agreement with the experimental values. The largest contribution (95%) to the a -dipole component comes from the four triply bonded monomers. Because of the relative rigidity of these triply bonded monomers, the averaged a -dipole projections are unlikely to be significantly altered upon intermolecular vibrational excitation, thereby yielding μ_a' and μ_a'' with the same sign as determined in our Stark measurements.

Ab initio calculations produce dipole moments only for the static equilibrium structures, and the experiments measure the vibrationally averaged values. To treat the vibrational-averaging effects explicitly, we used the rigid-body diffusion quantum Monte Carlo method (4, 20) together with the induction model for the dipole moment surface. This calculation gave a total dipole moment for the cage hexamer of 2.05 D, which is an enhancement of 8%. However, μ_a was correspondingly 5% smaller, giving a value of 1.89 D, which is in good agreement with the measured ground-state experimental value of 1.85 D.

We applied the iterated induction model to compute the individual monomer dipole moments in the clusters, and these results compare very well with the ab initio values (Fig. 3). The monomer dipoles in the hexamer cage structure deviate from the exponential enhancement trend exhibited by the dimer and the cyclic clusters; this result closely parallels the departure of the average O-O separation ($R_{\text{O-O}}$) for the cage (2.82 Å) from the value for the cyclic hexamer (2.76 Å) extrapolated from the exponentially contracting $R_{\text{O-O}}$ trend observed for the dimer and ring clusters (6, 27). Both trends identify the hexamer as the transition wherein three-dimensional hydrogen-bonded networks become more stable than the cyclic forms. The cage has the same

Fig. 2. The fully resolved experimental and simulated $\Delta M = 0$ electric field splitting patterns of the $P(4)$ VRT transitions of the cage hexamer (corresponding to $J' = K_a' = 3 \leftarrow J'' = K_a'' = 4$, where J is the quantum number of the overall angular momentum and K_a is its projection along the approximate symmetry axis) at an electrical field of 40.2 V/cm (top). The field-free patterns are given for comparison (bottom). Stark transitions arising from four disparate tunneling symmetries (A_a , A_b , B_a , and B_b) correlating to different nuclear spin states of the cluster were deconvoluted into three sets of stick spectra for each field; the middle stick spectrum contains two overlapping tunneling components ($A_b + B_a$). The relative intensities between the different symmetry species are proportional (20) to their nuclear-spin statistical weights as 19 (A_a): 6 + 6 ($A_b + B_a$): 2 (B_b). Individual M components are labeled, M being the magnetic quantum number corresponding to the projection of the total angular momentum J along the space-fixed axis defined by the electric field vector.

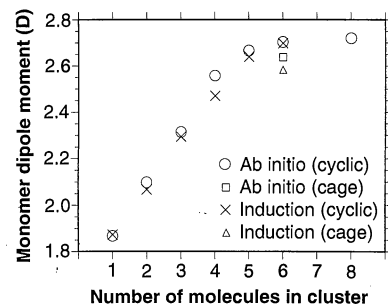
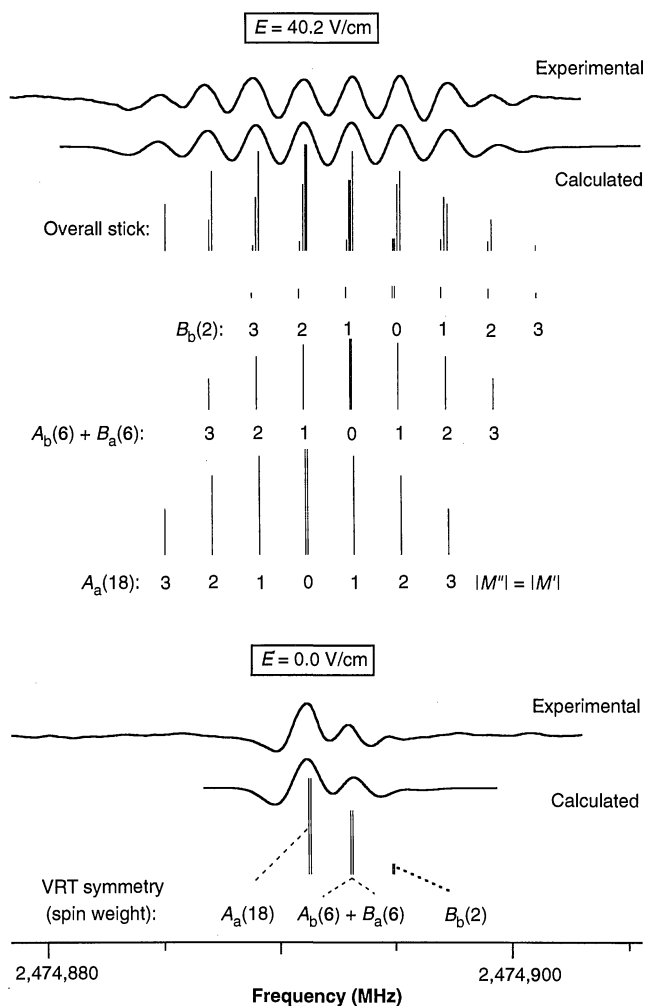


Fig. 3. Plot of the average dipole moment of a water monomer in a cyclic water cluster against the number of water molecules in the cluster. Ab initio and induction model results are shown. For the hexamer, dipoles for both the cage and cyclic structures are given. The octamer value is for the cubic (D_{2h}) structure.

structural arrangement as the basic unit of ice VI, for which R_{O-O} is 2.81 Å (28).

Finally, we used the induction model to calculate the monomer dipoles in a collection of 160 water molecules arranged into the lattice structure of ice I_h , which is currently beyond high-quality ab initio calculations. We obtained an average monomer dipole of 2.76 D for this model of ice I_h , compared with a value of 2.70 D calculated for the cyclic hexamer. The effective dipole moment of a water monomer in liquid water at 0°C is 2.4 to 2.6 D and should increase when the material becomes supercooled (29).

The close agreement achieved between the ab initio dipole moment enhancements and those computed from the induction model, together with the good agreement of the calculated vibrationally averaged μ_a for the cage hexamer with experiment, confirm the accuracy of the simple induction model for describing the dipole moments of water clusters. Our findings should facilitate the development of refined molecular models for liquid water. Furthermore, the close resemblance of the properties of the water hexamer with those of the condensed phases may indicate that the dominant interactions that occur in condensed-phase environments are reasonably well represented in even this small cluster.

REFERENCES AND NOTES

- N. Pugliano and R. J. Saykally, *J. Chem. Phys.* **96**, 1832 (1992); *Science* **257**, 1937 (1992); J. D. Cruzan *et al.*, *ibid.* **271**, 59 (1996); K. Liu, M. G. Brown, J. D. Cruzan, R. J. Saykally, *ibid.*, p. 62.
- K. S. Kim, M. Dupuis, G. C. Lie, E. Clementi, *Chem. Phys. Lett.* **131**, 451 (1986); C. J. Tsai and K. D. Jordan, *ibid.* **213**, 181 (1993); M. Schütz, T. Bürgi, S. Leutwyler, H. B. Bürgi, *J. Chem. Phys.* **99**, 5228 (1993).
- S. S. Xantheas and T. H. Dunning, *J. Chem. Phys.* **99**, 8774 (1993); S. S. Xantheas, *ibid.* **100**, 7523 (1994); *ibid.* **102**, 4505 (1995).
- J. K. Gregory and D. C. Clary, *ibid.* **102**, 7817 (1995); *ibid.* **103**, 8924 (1996); *ibid.* **105**, 6626 (1996).
- I. Ohimine, *J. Phys. Chem.* **99**, 6767 (1995).
- K. Liu, J. D. Cruzan, R. J. Saykally, *Science* **271**, 929 (1996).
- J. E. Del Bene and J. A. Pople, *J. Chem. Phys.* **52**, 4858 (1970); A. Raham and F. H. Stillinger, *J. Am. Chem. Soc.* **95**, 7943 (1973); R. J. Speedy, J. D. Madura, W. L. Jorgensen, *J. Phys. Chem.* **91**, 909 (1987); G. Corongiu and E. Clementi, *J. Chem. Phys.* **98**, 2241 (1993).
- F. J. Lovas, *J. Phys. Chem. Ref. Data* **7**, 1445 (1978).
- C. A. Coulson and D. Eisenburg, *Proc. R. Soc. London Ser. A* **291**, 454 (1966).
- D. J. Adams, *Nature* **293**, 447 (1981); M. I. Heggie, C. D. Latham, S. C. P. Maynard, R. Jones, *Chem. Phys. Lett.* **249**, 485 (1996); D. Wei and D. R. Salahub, *ibid.* **224**, 291 (1994).
- J. Caldwell, X. D. Liem, P. A. Kollman, *J. Am. Chem. Soc.* **112**, 9144 (1990); M. Sprik, *J. Chem. Phys.* **95**, 6762 (1991).
- K. Laasonen, M. Sprik, M. Parrinello, R. Car, *J. Chem. Phys.* **99**, 9080 (1993).
- I. Tuñón, M. T. Martins-Costa, C. Millot, M. F. Ruiz-López, *J. Mol. Model.* **1**, 196 (1996).
- R. D. Amos, CADPAC: Cambridge Analytical Derivatives Package (University of Cambridge Cambridge, 1992), version 5.
- A. J. Stone, *Chem. Phys. Lett.* **83**, 233 (1981);

- _____ and M. Alderton, *Mol. Phys.* **56**, 1047 (1985).
- R. A. Kendall Jr., T. H. Dunning, R. J. Harrison, *J. Chem. Phys.* **96**, 6796 (1992).
 - C. Möller and M. S. Plesset, *Phys. Rev.* **46**, 618 (1934).
 - K. Kim and K. D. Jordan, *J. Phys. Chem.* **98**, 10089 (1994).
 - T. R. Dyke, K. M. Mack, J. S. Muentner, *J. Chem. Phys.* **66**, 498 (1977).
 - K. Liu, *et al.*, *Nature* **381**, 501 (1996).
 - K. Kim, K. D. Jordan, T. S. Zwier, *J. Am. Chem. Soc.* **116**, 11568 (1994).
 - R. J. Saykally and G. A. Blake, *Science* **259**, 1570 (1993).
 - G. A. Blake *et al.*, *Rev. Sci. Instrum.* **62**, 1701 (1991); K. Liu *et al.*, *ibid.* **67**, 410 (1996). The Stark field was applied either between the nozzle and an electroformed metal screen in front of the molecular jet or to a pair of parallel hand-polished Al plates aligned horizontally to be parallel to the planar supersonic expansion, allowing $\Delta M = 0$ or $\Delta M = \pm 1$ type of

- transitions to occur, respectively. The tunable terahertz laser radiation was polarized in the horizontal plane.
- H. Linnartz, A. Kips, W. L. Meerts, M. Havenith, *J. Chem. Phys.* **99**, 2449 (1993).
- W. F. Murphy, *ibid.* **67**, 5877 (1977).
- J. Verhoeven and A. Dymanus, *ibid.* **52**, 3222 (1970).
- K. Liu, M. G. Brown, M. R. Viant, J. D. Cruzan, R. J. Saykally, *Mol. Phys.* **89**, 1373 (1996).
- S. W. Peterson and H. A. Levy, *Acta Crystallogr.* **10**, 70 (1957).
- D. Eisenberg and W. Kauzmann, *The Structure and Properties of Water* (Oxford Univ. Press, New York, 1969).
- The Berkeley authors (K.L., M.G.B., and R.J.S.) were supported by the NSF Experimental Physical Chemistry Program (CHE-9424482). The work in London and Cambridge was supported by the Engineering and Physical Sciences Research Council.

10 October 1996; accepted 29 November 1996

On the Quantum Nature of the Shared Proton in Hydrogen Bonds

Mark E. Tuckerman, Dominik Marx, Michael L. Klein, Michele Parrinello

The relative influence of thermal and quantum fluctuations on the proton transfer properties of the charged water complexes $H_5O_2^+$ and $H_3O_2^-$ was investigated with the use of ab initio techniques. These small systems can be considered as prototypical representatives of strong and intermediate-strength hydrogen bonds. The shared proton in the strongly hydrogen bonded $H_5O_2^+$ behaved in an essentially classical manner, whereas in the $H_3O_2^-$ low-barrier hydrogen bond, quantum zero-point motion played a crucial role even at room temperature. This behavior can be traced back to a small difference in the oxygen-oxygen separation and hence to the strength of the hydrogen bond.

Proton transfer through a hydrogen bond is a ubiquitous phenomenon, influencing dynamical behavior in a wide variety of systems ranging from materials science to biochemistry. For example, charge-conducting "water wires" (1) are crucial in the function of membrane protein channels (2), and the photosynthetic reaction center utilizes proton transduction in one of its fundamental steps (3). The strength and symmetry of the hydrogen bond are key properties that are often qualitatively correlated with its average length (4). Indeed, many living systems modulate the strength of hydrogen bonds (5, 6) and even promote hydrogen tunneling (7) to affect processes like enzyme catalysis. Despite its widespread importance, the quantum character of proton transfer has not been satisfactorily elucidated. This deficiency persisted because of the complexity of treating the thermal and quantum fluctuations of many atoms in conjunction

with a highly accurate description of both the strong and weak interactions (8). Accordingly, the focus has been on assessing zero-temperature quantum effects in simple model systems that often have a severely reduced dimensionality. Despite these restrictions, considerable knowledge has been accumulated (9).

In this report ab initio techniques are used to explore the quantum character of the shared proton in the hydrogen-bonded complexes $H_5O_2^+$ and $H_3O_2^-$ at room temperature. These complexes can be considered as prototypes of strong and intermediate-strength hydrogen bonds. Research on weakly bound aggregates like small neutral (10) or charged (11) water complexes has recently matured as a result of experimental progress. Generally, experimental and theoretical studies have focused more on $H_5O_2^+$ than on $H_3O_2^-$. Quantum chemical calculations at the Hartree-Fock level predict asymmetric bonding with one covalent OH bond as the most stable configuration for $H_5O_2^+$, suggesting that the proton moves on a potential with a double-well structure. This configuration corresponds schematically to $[H_2O-H^*...OH_2]^+$ and

M. E. Tuckerman and M. L. Klein, Center for Molecular Modeling and Department of Chemistry, University of Pennsylvania, Philadelphia, PA 19104-6323, USA.
D. Marx and M. Parrinello, Max-Planck-Institut für Festkörperforschung, Heisenbergstrasse 1, 70569 Stuttgart, Germany.